ON THE DESIGN OF STEEL FIBER REINFORCED CONCRETE TUNNEL LINING SEGMENTS

L. SORELLI[1,2], F. TOUTLEMONDE[2]

[1] Department of Civil Engineering, University of Brescia (Italy)

[2] Structural Division, Laboratoire Central des Ponts et Chaussées (France)

ABSTRACT

The structural applications of Steel Fiber Reinforced Concrete (SFRC) have recently been increasing due to the improvement of material properties, such as in the material toughness under tension and durability. However, because the behavior of such structures is fairly different from conventional Reinforced Concrete (RC) structures the classic design method should be critically reviewed considering the post-cracking resistant mechanism.

This work focuses on the application of SFRC in tunnel lining segments, as an alternative to conventional RC segments. Based on an accurate experimental investigation on full scale specimens, a smeared crack model, which implements the Hilleborg's criteria was used.

In order to assess the SFRC reliability, a wide population of tensile tests on cylinders drilled out from a reference full scale specimen was carried out. The tensile constitutive relation, which is the fundamental property for SFRC materials, was chosen on a probabilistic fashion accounting for the actual dispersions of fiber in the tunnel segment due to the casting procedure. According to the finite element analysis, the structural response of such structures was found to be very sensitive to the fiber dispersion.

Finally, the AFREM recommendation for SFRC materials and the simplified 'struts and ties' model were evaluated by means of a parametric analysis.

1. INTRODUCTON

The steel fiber reinforcement not only improves the toughness material, the impact and the fatigue resistance of concrete, but it also increases the material resistance to cracking and, hence to water and chloride ingress with significant improvement in durability of concrete structures. Therefore, the use of SFRC in tunnel structures represents an attractive technical solution with respect to the conventional steel reinforcement, because it reduces both the labor costs (e.g. due to the placement of the conventional steel bars) and the construction costs (e.g. forming and storage of classical reinforcement frames, risks of spalling during transportation and laying).

For these reasons several European pilot projects have been undertaken to assess the reliability of SFRC in tunnel structures, as examples the 2nd Heinenoord tunnel (Netherlands) [1] and the two SFRC tunnel linings in Essen and Ruhr-Region (Germany) [2]. These preliminary SFRC examples exhibited reduced crack development and a lower risk of leakage and the falling off of concrete flakes, which often represents a concrete issue for tunnel road. Furthermore, the steel fiber reinforced details, such as the shear tooth of ring joints, was found to exhibit a higher ductility under localized force.

Due to the current lack of design rules for Steel Fibers Reinforced Concrete (SFRC) structures, engineers have usually designed SFRC tunnel lining segments by adopting the same rules that are valid for concrete with conventional reinforcement. However, the post-cracking behavior of SFRC structure is dramatically different from conventional RC structures. After the cracking onset, SFRC structures exhibit a markedly non-linear behavior to the extend that strain softening behavior may occur with the fiber volume fraction frequently used in practice ($V_f = 0.3$-0.6%; Figure 1a). On the other hand, the conventional reinforcement keeps an almost linear behavior (with a lower stiffness with respect to the uncracked stage) until the reinforcement yields (Figure 1b). It is possible to reproduce the actual behavior of SFRC structures from the

[Extended abstract]

crack onset up to the collapse mechanism by considering the fiber contribution (bridging effect) in the tensile behavior with Non Linear Fracture Mechanics (NLFM) based methods. In this way SFRC tunnel linings can be more correctly designed for both the serviceability and the ultimate state preventing excessive deformations and cracking development which could compromise the serviceability along with the durability of such structures. Moreover, the post-cracking behavior of SFRC structures could further increase the ultimate load in the case of hyperstatic structures, where after initial plasticity the redistribution of forces occurs.
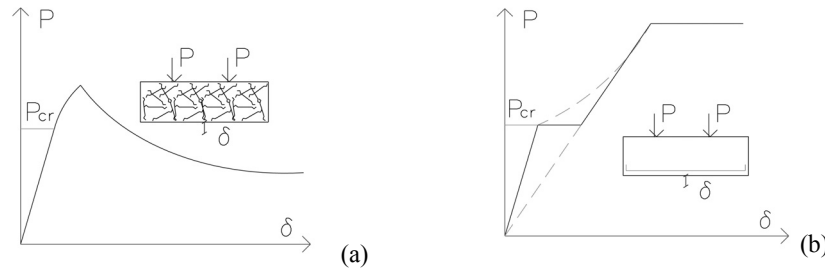

Figure 1. Typical response of a bending test on a SFRC beam (a) and on RC beam (b).

This work analyses the experimental results of extensive investigation on full-scale RC and SFRC precast tunnel segments recently carried out under a national project [3] by means of a crack band finite element model [4, 5]. The modeling was improved by taking into account the actual dispersion of fibers in the SFRC tunnel due to the flow direction, wall effect and gravitational force during the casting phase. Based on post-cracking tensile resistance measured on 36 cylinders drilled out from a full-scale reference specimen, the zones of the tunnel segment with an higher fiber concentration were distinctly recognized. By simply assuming different post-cracking tensile relations for these zones according to the experimental response, the fiber distribution was found to remarkable affect the global behavior of such SFRC structures.

Besides the validation of the finite element model for SRFC and RC tunnel structures, the AFREM design guidelines for SFRC materials [6] and the simplified 'struts ant tie' analysis method [7] are assessed by means of a parametric analysis.

In conclusion, the reliability of the structural response was evaluated by taking into account the constitutive tensile relation on a probabilistic base within a confidence interval, since the post-cracking behavior of SFRC (at low fiber content) is very sensitive to the content and distribution of the fibers and the inherent tensile response is usually characterized by a relative high dispersion.

2. EXPERIMENTS

Three SFRC segments (V1, V4, V5), and two RC (V2 and V3) were especially cast, in industrial conditions, for the experimental investigation. All the segments was full-scale samples with a inner diameter of 6.30 m, a thickness of 0.30 m and a length of 1.42 m (Figure 3).

The main experimental results are available in [3] along with mix-proportions, reinforcement details, and mechanical properties at 28 days. At the date of the test (11 months) the compressive strength of the of the plain concrete and the of the SFRC were 97.5 MPa and 74.2 MPa, respectively, while the Young's modulus were 49.7 GPa and 42.4 GPa. Furthermore, the SFRC was characterized under uniaxial tensile test on 36 cylindrical cores ($\phi = 140$ mm, L = 150 mm) drilled out from the specimen V1, following the directions of the major extension (Figure 2). The tensile tests were performed according to AFREM guidelines [6], which provide fixed boundary conditions and a crack opening rate of 5 μm/min measured by three clip gauges astride the notch (depth of 20 mm and thickness of 2 mm). Figure 2 shows the tensile response of all the cylinders

in terms of the tensile stress vs. crack opening displacement (σ-w). By displaying the average curves of the specimens drilled out from the same vertical section (columns A, B, C, D, E, F) or from the horizontal sections (rows 1, 2, 3, 4, 5, 6), it is observed the specimens belonging to the zones indicated as 'row 1' and 'column C' exhibit a systematic higher residual strength (Figure 2). The flow direction of the fresh concrete, which was pumped in the tunnel though a hole located in the center of the metallic mold has caused an uneven distribution of fibers in the specimen.

The tunnel lining segment was tested in a configuration that was considered to be critical for design and corresponded to the *in situ* laying extremely off-centered loading (Figure 3). The loads were applied by two hydraulic jacks inserted in a closed frame fixed to the strong floor of the laboratory. The supports were as widely apart as possible from the axis (3.15 m is the total span at the mid-surface) to maximize the bending moment. However, since the vertical reactions were not located in the same plane as the applied load, the toppling moment had to be balanced by horizontal support forces located in the vicinity of the zones where the vertical load was applied.
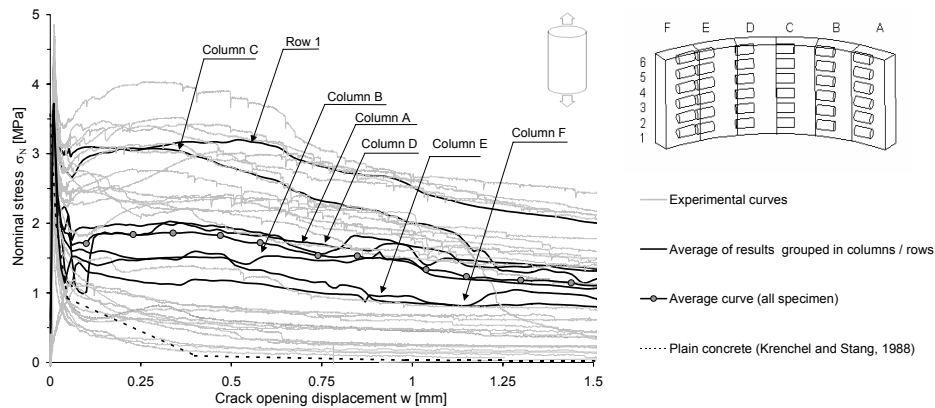

Figure 2. Experimental tensile test response in terms of stress-crack opening displacement σ_N-w.
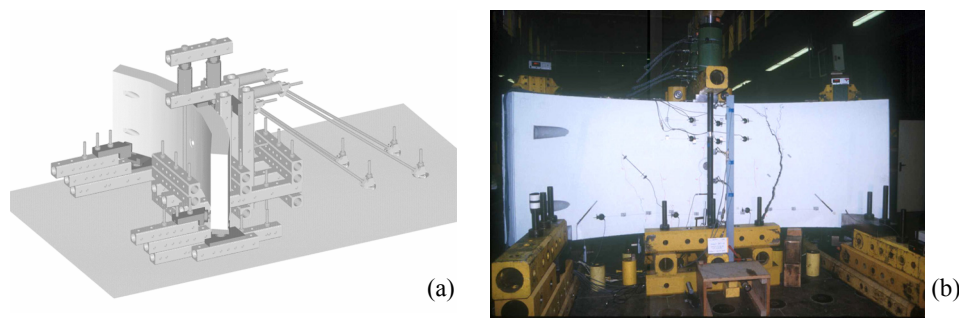

Figure 3. Scheme of the testing frame (a); crack development in a SFRC specimen (b).

3. FINITE ELEMENT MODEL

The crack band model accounts for the two main failure mechanics for concrete by two hardening variables with softening behavior in tension (cracking) and initial hardening followed by softening (crushing) in compression [4, 5]. A characteristic length, based on the Hilleborg's criterion, is introduced to reduce the sensitivity of the results to mesh density. The evolution equation of the

hardening variables are conventionally formulated by considering the uniaxial loading conditions first and then extended to multiaxial conditions.

The effect on the structural behavior of the tensile constitutive relation (σ-w), which is the fundamental property for SFRC, is here investigated. Therefore, different tensile constitute relations (σ-w) are considered in this work as shown in Figure 4a and listed in the following: (i) the average tensile relation from all the cylinders tested under uniaxial test (dotted circle line); (ii) the tensile relations averaged from the tensile response of the cylinders drilled out from the zones 'column C' and 'row 1', which were characterized by higher fiber distribution; (iii) the tensile law for SFRC material according to the AFREM recommendations (dotted square line), which are based on the characteristic value of the experimental fracture energy; (iv) the tensile relations corresponding to the confidence limits of 95% of the experimental tensile responses on SFRC cylinders (bold lines); (v) the theoretical tensile relation for the plain concrete proposed by Krenchel and Stang [8] (dotted triangle line), which models the aggregate interlocking in mode-I crack opening.

The Young's modulus and the Poisson's ratio elastic mechanical properties are experimentally determined, while the uniaxial compressive behavior (σ-ε) was deduced from PrEN 1992-1-1 basing on the experimental compressive strength (f_c).

The finite element mesh, which models half of the specimen, was composed as uniform as possible by 14000 nodes and 11391 linear brick elements (Figure 4b). In the case of RC specimen, the steel bars were modeled by means of 591 two-nodes truss element and the material behavior for the steel bar was elastic-plastic with yield strength of 550 MPa. For simplicity, it is assumed a perfect bond between concrete and steel bar. The boundary conditions representing the external testing frame are modeled by elastic springs, of which the elastic stiffness is calibrated on the experimental data.
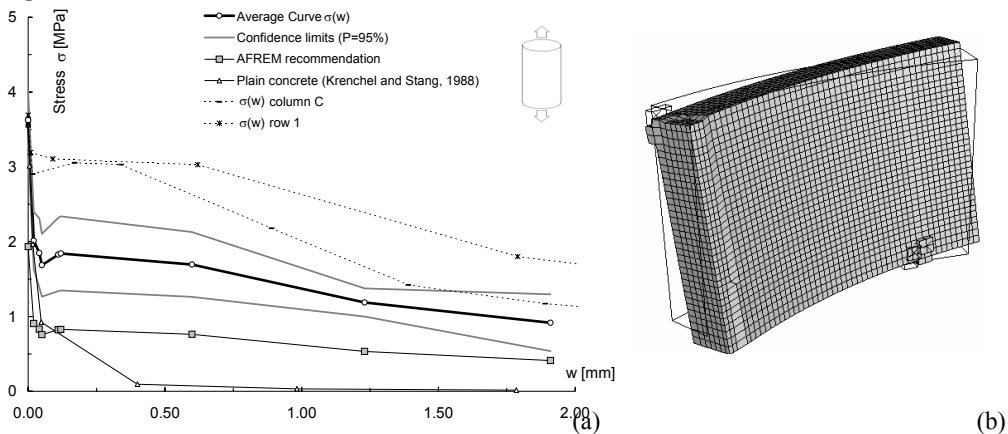

Figure 4. Tensile relstions (σ-w) adopted (a); deformed mesh for SFRC segment (b).

4. RESULTS AND CONCLUSIONS

Figures 4a and 4b show the experimental and numerical responses for the SFRC and RC specimens, respectively, in terms of vertical load and mid-span deflection. In the former case, the model captures the first crack point and the overall behavior well, with a slight underestimation of the peak load. However, by considering the material heterogeneity due to the uneven fiber distribution , i.e. adopting the specific tensile laws for the zones previously called 'column C' and 'row 1', the numerical solution better fits the experimental peak load. The load test control caused a very brittle collapse, while the numerical analyses, which were performed with the arc length

numerical analysis technique, better follow the equilibrium path showing a remarkable residual strength after the peak-load (Figure 4a). At the collapse, a major crack propagated vertically on the inner side in the proximity of the mid-span in fair accordance to the experimental evidence.

In the case of the RC specimens the numerical response predicts an accurate enough peak load, but the global response appears to be stiffer due to the perfect bond assumption (Figure 4b). The finite element model confirms a ductile collapse due to the plastic failure of the inner side steel bars and the five lowest rebars of the outer side.
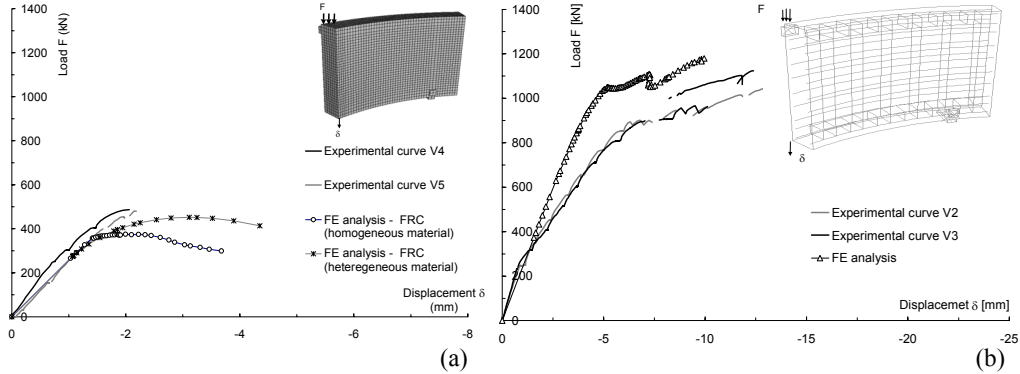

Figure 5. Experimental and numerical responses of the SFRC (a) and of the RC specimens (b).

The goodness of the struts and tie model as formulated in [7] is evaluated by means of the finite element model by assuming different loading positions. Figure 5 shows the numerical load displacement curve for different span length (S = 1708 mm, 2472 mm, 3149 mm). As expected the reduction of the span length causes a greater peak load and the structural behavior tends to become more brittle until the snap-back phenomena occurs. Nevertheless, the residual strength for the SFRC specimen can still be observed. The evaluation of the ultimate load by the simplified 'struts and tie' analysis, which assumes the tensile stress is localized at the bottom third of the cross section at mid-span, appears to be in good agreement with the finite element models (Figure 5b).
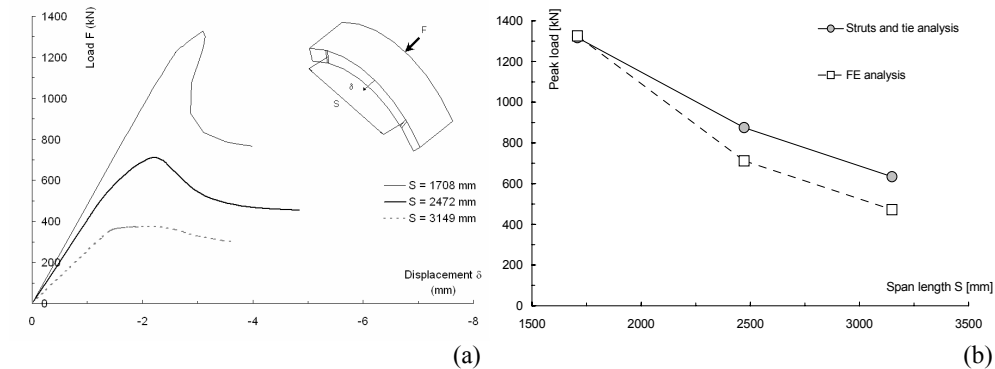

Figure 6. Load position effect on the structural response of the SRC tunnel (a) and the comparison between the numerical and the simplified design method prediction in terms of peak load (b).

Finally, the structural behavior correspondent to each one of the different tensile law (σ-w) above considered is evaluated by the finite element model. The results are shown in Figure 7 in terms of load and displacement of the mid-span section. The AFREM recommendation provided a

safe factor in terms of ultimate load of approximately 2. By comparing the structural behavior of the segments made of plain concrete and SFRC, which are characterized by the same tensile strength, the significant enhancement of the ultimate load and the dissipated is noticed. Figure 7b displays the effect of the fracture energy of the tensile laws herein adopted on the ultimate load of tunnel segment axially loaded.
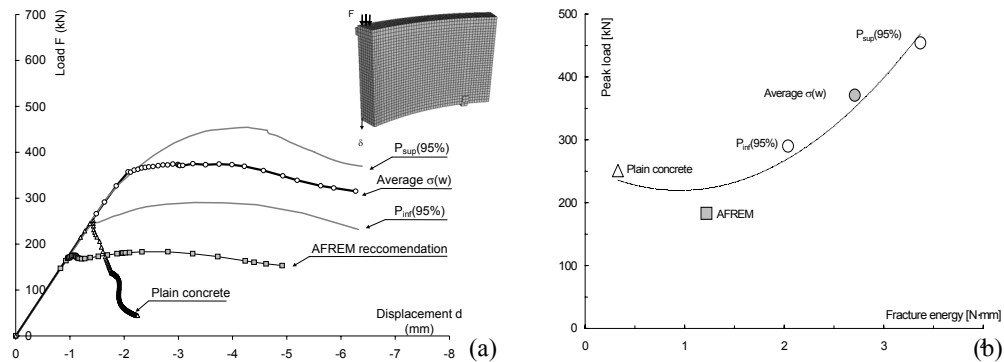

Figure 7. Confidential limits, design curve according to AFREM and plain concrete σ-COD curves (a) and the correspondent structural behavior (b).

In conclusion, SFRC design reliability requires a confident evaluation of the tensile constitutive relation, which is usually characterized by a high dispersion. AFREM recommendation provided a safe prediction of the ultimate load. In addition, the simplified 'struts and tie' analysis, which is usually used for RC structures, can be also adapted to the SFRC tunnels design by properly considering the tensile resistance of the material in the collapse mechanism.

REFERENCES
1. Kooiman, A.G., and Walraven, J. *'Steel Fibre Reinforced Concrete Segments in the Second Heinenoord Tunnel'*. in *fib Symposium*. 1999. Prague, Czech Republic,.
2. Schnütgen, B. *'Design of Precast Steel Fibre Reinforced Tunnel Segments'*. in *Proc., RILEM TC 162-TDF Workshop*. 2003. Bochum (Germany).
3. Toutlemonde, F., Quiertant, M. and Petit, F., *Revêtements et soutènements. Voussoirs de Tunnel préfabriqués*, in *Le développment industriel des BÉtons de FIbres Métalliques. Conclusions and reccomandations*, Press ENPC, Editor. 2002.
4. Lubliner, J., J. Oliver, S. Oller, and E. Oñate, *'A Plastic-Damage Model for Concrete'*. International Journal of Solids and Structures, 1989. **25**(3): p. 229-326.
5. ABAQUS/STANDARD, *User's Manual, Hibbitt, Karlsson & Sorensen, Inc., Pawtucket*. 1995:
6. Rossi, P., *'Les bétons de fibres metalliques: Méthodes de dimensionnement Essais de Caractérisation, de convenance et de contrôle'* Association Francaise de Recherches et d'Essais sur le materiaux et les Constructions (AFREM): 1995, Saint Remy Les Chevreuse. p. 73.
7. Toutlemonde, F., *'Analyse des résultats des essais de voussoirs de tunnel par des méthodes de dimensionnement approchées'*. 2000, National Project BEFIM, report, LCPC.
8. Krenchel, H., and Stang, H. *'Stable Microcracking in Cementitious Materials'*. in *Brittle Matrix Composites, Proceedings Second International Symposium on Brittle Matrix Composites*. 1988. (BMC2), Poland.